LBL--15162

DE83 003591

LBL-15162

NUCLEAR MOMENTS OF INERTIA AT HIGH SPIN

M.-A. DELEPLANQUE

Nuclear Science Division, Lawrence Berkeley Laboratory,
University of California, Berkeley, CA 94720

Presented at the Conference on High Angular Momentum
Properties of Nuclei, Oak Ridge, TN, November 2-4, 1982

This work was supported by the Director, Office of Energy Research, Division of Nuclear Physics of the Office of High Energy and Nuclear Physics of the U.S. Department of Energy under Contract DE-AC03-76SF00098.

NUCLEAR MOMENTS OF INERTIA AT HIGH SPIN

M.-A. DELEPLANQUE
Nuclear Science Division, Lawrence Berkeley Laboratory, University of California, Berkeley, CA 94720

Abstract The competition between collective motion and alignment at high spin can be evaluated by measuring two complementary "dynamic" moments of inertia. The first, $\mathcal{J}^{(2)}$, measured in γ-γ correlation experiments, relates to the collective properties of the nucleus. A new moment of inertia $\mathcal{J}^{(2)}_{eff}$ is defined here, which contains both collective and alignment effects. Both of these can be measured in continuum γ-ray spectra of rotational nuclei up to high frequencies. The evolution of γ-ray spectra for Er nuclei from mass 160 to 154 shows that shell effects can directly be observed in the spectra of the lighter nuclei.

INTRODUCTION

Even rotational nuclei do not rotate like a rigid body. Instead the angular momentum is generated both by "collective" rotation of the nucleons and by "alignment" of some single-particle angular momentum along the rotation axis. In such nuclei, the alignment of a few high-j orbitals is produced by the Coriolis and centrifugal forces. At "low" spin (<40$\hbar$), the contribution from "aligned" particles is dominant in nuclei near the major closed shells (for example ^{152}Dy, ^{150}Gd), whereas the collective contribution is more important near the middle of shells (as in ^{164,160,158}Er). But in any case, the

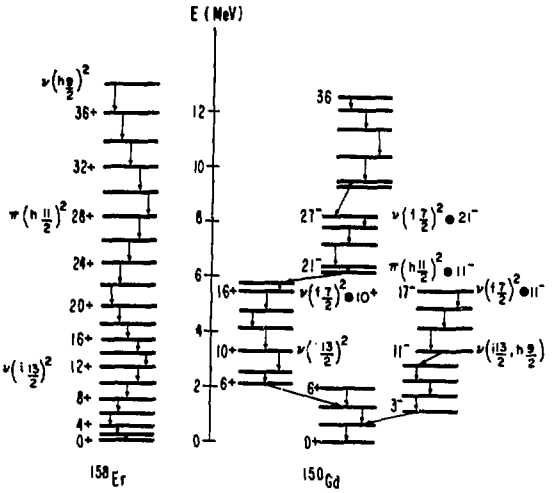

XBL 8210 1283

FIGURE 1. Partial level schemes of ^{158}Er and ^{150}Gd nuclei. The aligned configurations are indicated.

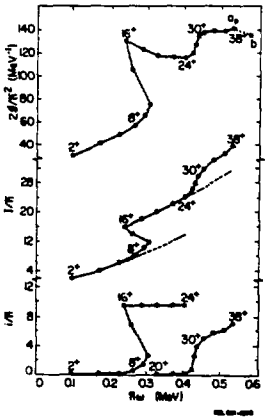

FIGURE 2. Plots of the moment of inertia $\mathcal{J}^{(1)}_{eff}$, of the total spin I and of the alignment i as a function of frequency for the nucleus ^{158}Er.

alignments are the manifestation of single-particle orbitals that play a special role because of their high angular momentum. In ^{150}Gd, for instance (Figure 1),[1] the states up to about 30$\hbar$ can be described approximately by aligned, near-spherical shell model configurations. In contrast, in more collective nuclei like ^{158}Er (Figure 1), about half the angular momentum arises from alignment of a few high-j quasiparticles: $\nu i_{13/2}$, $\nu h_{9/2}$, $\pi h_{11/2}$.

At low spin in quasirotational nuclei those two components are rather easy to distinguish through discrete line studies and a plot of spin I as a function of rotational frequency ω, defined as $\hbar\omega = dE/dI$, where E is the excitation energy of the nucleus. In nuclei where the stretched quadrupole transitions are predominant, $\hbar\omega$ is experimentally accessible, since it is approximately half the γ-ray transition energy E_γ. The smooth, regular increase of spin I with frequency corresponds to a collective rotation whereas the sharp increase of spin in narrow frequency regions is caused by sudden alignment of the angular momentum of some specific orbitals on the rotation axis. Thus in ^{158}Er (Figure 2), the region of spin between 16^+ and 24^+ represents a collective band constructed on a $(\nu i_{13/2})$ two-quasiparticles state. It crosses the ground band in the spin region 10-16 and in the frequency region around $\hbar\omega \simeq 0.28$ MeV. The change i in the nuclear alignment at that crossing is approximately[2] the difference between the spins in the two "unperturbed" bands at a given frequency. There are two more crossings known in the yrast sequence of ^{158}Er: one is due to the alignment of a pair of protons in $h_{11/2}$ orbits around $\hbar\omega \simeq 0.43$ MeV and the other is very likely[3]

caused by the alignment of a neutron pair in $h_{9/2}$ orbits, around $\hbar\omega \approx 0.5$ MeV.

Above spin 40, such a detailed analysis cannot at present be performed because individual bands are no longer seen. Instead of being mainly concentrated in a few bands close to the yrast line, the γ-ray intensity is spread over many decay paths and gives rise to a "continuum" spectrum. One of the interesting questions is whether single-particle effects still play a significant role in generating angular momentum. But, for the experimental reasons just mentioned, this problem must be addressed differently, through the notion of moments of inertia.

TWO BASIC MOMENTS OF INERTIA AT HIGH SPINS

It has been realized for some time[2] that there are two general kinds of moments of inertia, the kinematic moments of inertia, which are related to the overall motion of the nucleus, and the dynamic moments of inertia, which describe its response to a torque.

For a perfect rotor with a moment of inertia $\mathcal{J}$, the rotational energy at spin I is $E = \hbar^2/2\mathcal{J}\, I^2$. Its first derivative with respect to spin:

$$\frac{dE}{dI} = \frac{\hbar^2 I}{\mathcal{J}} = \frac{E_\gamma}{2} = \hbar\omega$$

is related to the kinematic moment of inertia $\mathcal{J}^{(1)}$ defined as

$$\frac{\mathcal{J}^{(1)}}{\hbar^2} = I\left(\frac{dE}{dI}\right)^{-1} = \frac{I}{\hbar\omega}$$

NUCLEAR MOMENTS OF INERTIA AT HIGH SPIN

The second derivative

$$\frac{d^2E}{dI^2} = \frac{\hbar^2}{\mathcal{J}} = \hbar \frac{d\omega}{dI}$$

is related to a dynamic moment of inertia $\mathcal{J}^{(2)}$:

$$\frac{\mathcal{J}^{(2)}}{\hbar^2} = \left(\frac{d^2E}{dI^2}\right)^{-1} = \frac{1}{\hbar}\frac{dI}{d\omega}$$

$\mathcal{J}^{(2)}$ represents the rate of change in spin with frequency. Those two moments of inertia are identical for a perfect rotor. But when there are changes in the internal structure of the nucleus, such as alignment of single-particle angular momentum, I/ω will be different from $dI/d\omega$ reflecting the fact that the nuclear motion is not the simple rotation of a rigid body. A schematic example of a typical decay path is shown in Figure 3. It is a translation, on an E versus I diagram, of a curve of the type shown in Figure 2. $\mathcal{J}^{(1)}$ and $\mathcal{J}^{(2)}$ can be defined for any sequence of levels, and I would like to introduce two of them here, since they prove to be the

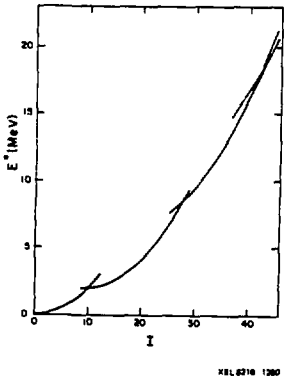

FIGURE 3. Schematic decay path of a nucleus on an excitation energy versus spin plot.

most significant ones for high spin studies. A number of recent experiments[4] suggest that up to the highest spins, a decay path consists of a succession of "collective" bands based on quasiparticle levels having different alignments. The collective motion can then be characterized by a "band" moment of inertia $\mathcal{J}^{(2)}_{band} = (dI/d\omega)_{band}$. It is accessible experimentally at high spins through the γ-γ correlation method that "identifies" in-band transitions. $\mathcal{J}^{(2)}_{band}$ is measured as a function of frequency and represents an average value over many bands at that frequency. Although data with better statistics are needed, it seems that in general $\mathcal{J}^{(2)}_{band}$ tends to decrease at high frequencies (which is also at high spins in quasirotational nuclei), suggesting a decrease in the collectivity of nuclear motion.

I want now to introduce a moment of inertia that I shall call $\mathcal{J}^{(2)}_{eff}$ and that will include both collective motion and alignment effects. The reason is that we recently realized that we could measure such moments of inertia at high spins (frequencies) and therefore try to estimate single-particle effects by comparing them with $\mathcal{J}^{(2)}_{band}$ values.

$\mathcal{J}^{(2)}_{eff}$ is defined as $(dI/d\omega)_{path}$. For the single path of Figure 3, it is the same as $\mathcal{J}^{(2)}_{band}$ in the band regions, but is also defined in the crossing frequency region, where it can take very large values. $\mathcal{J}^{(2)}_{eff}$ describes how easily angular momentum is generated when the rotational frequency increases. The increase of total angular momentum ΔI in a frequency region $\Delta\omega$ can be separated into a collective contribution ΔI_{band} and some contribution Δi from alignment.

NUCLEAR MOMENTS OF INERTIA AT HIGH SPIN

Therefore $\frac{\Delta I}{\Delta\omega} = \frac{\Delta I_{band}}{\Delta\omega} + \frac{\Delta i}{\Delta\omega}$, and with our definitions

$$\frac{\Delta i}{\Delta I} = 1 - \frac{\mathcal{J}^{(2)}_{band}}{\mathcal{J}^{(2)}_{eff}}$$

By measuring $\mathcal{J}^{(2)}_{band}$ and $\mathcal{J}^{(2)}_{eff}$ one can hope to learn about the contribution of the alignment to the spin as a function of frequency.

Apart from feeding effects (discussed later), the height of the continuum γ-ray spectrum of a quasirotational nucleus, decaying after a compound nucleus reaction, is a measure of the moment of inertia $\mathcal{J}^{(2)}_{eff}$: the γ-ray transitions are predominantly stretched E2 so that the rotational frequency is $\hbar\omega = E_\gamma/2$, and the spectrum is normalized to the γ-ray multiplicity so that the number of transitions per unit spin interval is $dN/dI = 1/2$. The height of the spectrum (as a function of ω) is $\frac{dN(\omega)}{d\omega} = \frac{dN}{dI}\frac{dI(\omega)}{d\omega} \simeq \frac{1}{2}\frac{dI}{d\omega}$, directly proportional to $\mathcal{J}^{(2)}_{eff}(\omega)$. The value of $\mathcal{J}^{(2)}_{eff}$ at a frequency ω is also an average over the contributions of all the paths decaying from a selected population of entry states. For instance, in our case, those states are selected by taking slices of total γ-ray energy.

HIGH SPIN BEHAVIOR OF ROTATIONAL NUCLEI

An "isotropic" continuum γ-ray spectrum is shown in Figure 4. It samples the decay of high spin states in the $^{124}Sn + ^{40}Ar$ at 185 MeV. The exponential high-energy part corresponds to the tail of a statistical spectrum

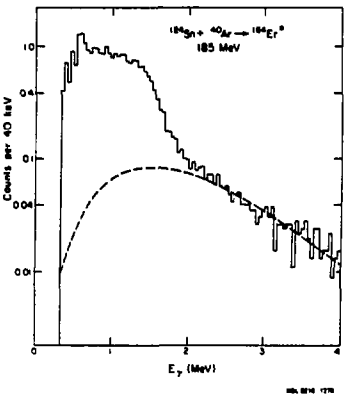

FIGURE 4. "Isotropic" γ-ray spectrum (histogram), normalized to the γ-ray multiplicity, from the deexcitation of high spin states of the compound nucleus ^{164}Er. The statistical part of the spectrum is shown as a dashed line.

that can be subtracted, assuming a shape of the form $E_\gamma^3 e^{-E_\gamma/T}$ with T = 0.5 MeV (dashed line). The remaining yrast part is composed mainly of stretched E2 transitions (see Figure 9, solid line). Except for incomplete feeding, it is proportional to $\mathcal{J}^{(2)}_{eff}$. Overall $\mathcal{J}^{(2)}_{eff}$ is roughly constant as expected for a reasonably good rotor. It is interesting to look at that spectrum in some more detail.

The low energy part of the spectrum shows some structures, most of which are known from discrete lines studies. The large peak around $E_\gamma \approx 600$ keV is due to the first backbend in ^{160}Er, the 4n product of the reaction. It shows directly that in the frequency region 0.3 MeV, a large amount of angular momentum is generated by aligning a pair of $i_{13/2}$ neutrons on the rotation axis. The second peak at $E_\gamma \approx 750$ keV is the "blocked" backbend in ^{159}Er, the 5n product also present, and the third peak at $E_\gamma \sim 900$ keV is very probably the second backbend in ^{160}Er.

NUCLEAR MOMENTS OF INERTIA AT HIGH SPIN

The effect of incomplete feeding at high spins is seen in Figure 5. It shows the yrast part of two spectra (as a function of frequency) for the same system, one from the decay of high spin entry states (solid line) and one from the decay of lower spin entry states (dashed line). They have about the same height but the "dashed" spectrum terminates at a lower frequency because the highest spins are not fed in that case. This shows that, on the average, the spin is proportional to frequency, and that the height at the edge of the bump is not proportional to $\mathcal{J}^{(2)}_{eff}$ because of incomplete feeding. So, if we can find to what extent the states that decay in a given frequency region are fed directly, we can then correct for the feeding and extract the value of $\mathcal{J}^{(2)}_{eff}$.

An approximate method[5] has recently been developed for that purpose. We consider an experiment where we look at continuum γ-ray spectra in NaI detectors as a function of different slices of total γ-ray energy detected in coincidence in a sum spectrometer. These continuum γ-ray spectra sample the decay paths from a variety of entry states selected by the total γ-ray energies. We shall first consider a schematic case. If we suppose that we know the spin population f(I) of entry states (Figure 6a, solid line) and that the γ-ray transitions are <u>all stretched quadrupole</u> we obtain the γ-ray spectrum as a <u>function of spin</u> of Figure 6b: since every state directly fed will decay through all the lower spin states, the spectrum height at a spin I (per cascade) is just the integral of the normalized feeding curve above spin I. In the region of spin that is fully fed, there will be half a transition per unit spin. For a spin feeding slightly shifted (Figure 6a, dashed line) but of

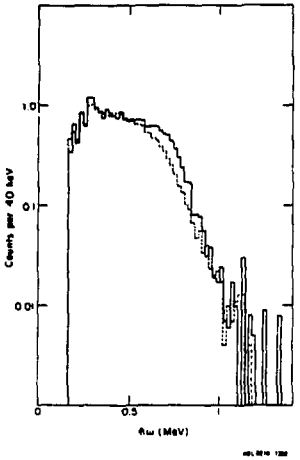

FIGURE 5. Yrast part of the spectrum of Figure 4 (solid line). The dashed line is the yrast part of a spectrum corresponding to a lower spin feeding for the same system.

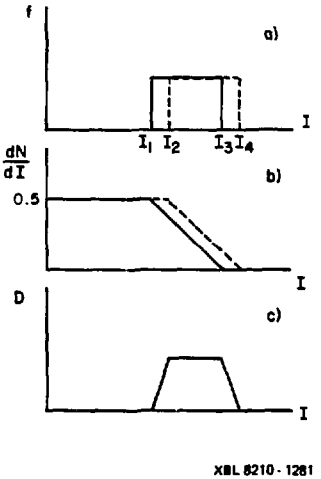

FIGURE 6. Schematic illustration of the feeding correction method: (a) two rectangular spin feeding curves, slightly shifted from each other. (b) the γ-ray spectra (as a function of spin) deexciting the populated states of (a). (c) the difference of the spectra of (b). It is used to correct the average spectrum of (b) for the feeding.

the same shape, the corresponding spectrum will be Figure 6b, dashed line. The difference D(I) of those two spectra (Figure 6c) is close to the average of the two spin feeding curves, so that it can be used to correct the average of the two spectra of Figure 6b. Therefore, to find the spectrum height dN/dI at spin I corresponding to full feeding, one will divide the average spectrum of Figure 6b by the normalized integral of the average spin feeding above spin I, or, to a good approximation, by the integral above spin I of the difference D(I) of the two spectra in Figure 6b. The same principle applies to experimental γ-ray spectra. At each frequency ω, the height of the (normalized) γ-ray spectrum is $\mathcal{J}^{(2)}_{eff}(\omega)dN/dI$ and their difference $d(\omega)$ (for two different feeding curves) is $\mathcal{J}^{(2)}_{eff}(\omega)D(I)\Delta I$, where ΔI is the average spin step from one feeding curve to the next[5]. If, on the average I is a monotonic function of ω, $I=g(\omega)$ (as is believed to be true in quasirotational nuclei), this means that the states lying above a certain spin $I_0=g(\omega_0)$ will also be above the corresponding frequency ω_0. This also means that D(I) can be expressed as a function of ω by $D(\omega) = D(I)(dI/d\omega) = \mathcal{J}^{(2)}_{eff}D(I)$, and therefore $d(\omega) = \Delta I D(\omega)$. This argument is the same whether $\mathcal{J}^{(2)}_{eff}$ is constant or not. It also follows from Figure 6 that using the difference spectrum will be a better approximation the smaller the spin step.

Figure 7 shows some $\mathcal{J}^{(2)}_{eff}$ spectra obtained after the correction for the feeding in three systems: $^{130}Te, ^{126}Te, ^{124}Sn + ^{40}Ar$ at 185 MeV, leading respectively to $^{166,165}Yb, ^{162,161}Yb$, and $^{160,159}Er$ as main products. Each curve shown is an average of three $\mathcal{J}^{(2)}_{eff}$ spectra obtained after correcting γ-ray spectra fed at low spin,

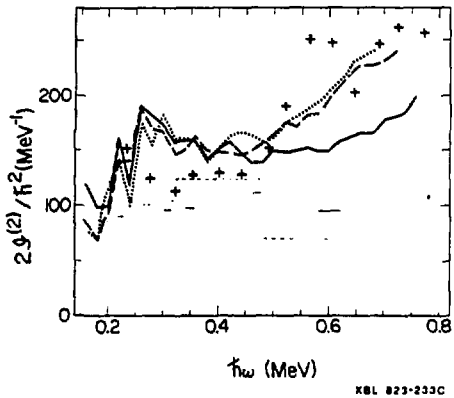

FIGURE 7. Moments of inertia $\mathcal{J}^{(2)}_{eff}$ (thick lines) as a function of frequency for the three systems = $^{130}Te + ^{40}Ar$ (dashed line), $^{126}Te + ^{40}Ar$ (dotted line), and $^{124}Sn + ^{40}Ar$ (solid line). Moments of inertia $\mathcal{J}^{(2)}_{band}$ (thin lines) for $^{130}Te + ^{40}Ar$ (dashed line) and $^{124}Sn + ^{40}Ar$ (solid line). Calculated $\mathcal{J}^{(2)}_{eff}$ [10] for $^{130}Te + ^{40}Ar$ (crosses).

high spin, and over a broad spin range. The new feature is that all these spectra exhibit a rise at high frequency, starting around 0.5 MeV for the ytterbium nuclei and 0.6 MeV for the erbium nuclei. This suggests that there exists a new way for the nucleus to generate angular momentum. Between 0.25 and 0.5 MeV in those spectra, there were already some peaks, most of them associated with known quasiparticle alignments. $\mathcal{J}^{(2)}_{band}$ values for $^{166,165}Yb$ and $^{160,159}Er$ deduced from discrete lines and γ-γ correlation data are shown as thin lines in Figure 7. In the low frequency region, the backbends are not asso-

ciated with high values of $\mathcal{J}^{(2)}_{band}$ since the gain in spin there proceeds through a few quasiparticle alignments and not by collective motion. The low values of $\mathcal{J}^{(2)}_{band}$ tentatively obtained[4,6] at high frequency also suggest the occurrence of alignments. The nuclei ^{166}Yb and ^{162}Yb, which have the same proton number, start aligning at the same frequency, whereas ^{160}Er and ^{162}Yb, which have the same neutron number, behave differently. This suggests that the protons are playing the more important role, probably populating aligned $i_{13/2}$ and $h_{9/2}$ orbitals, which are coming down to the Fermi level at these frequencies as calculated by several groups.[7,8] The filling of these high-j orbitals could also trigger an increase in deformation or a change of shape. A larger deformation might be expected to favor collective rotation over alignment, whereas the reverse would generally be true for a shift toward triaxial shape. Thus, the increased alignment discussed above and the lack of strong rotational features (valley and ridges) in the correlation spectra at these frequencies may suggest triaxial shapes. The filling of the $i_{13/2}$ and $h_{9/2}$ proton <u>particle</u> states (in contrast to the previously filled $i_{13/2}$ quasineutron and $h_{11/2}$ quasiproton orbitals, which are mixed <u>particle-hole</u> states) would tend to drive the system triaxial. Indeed, recent calculations by T. Bengtsson and I. Ragnarsson,[9] for ^{166}Yb where they follow a given configuration as a function of frequency, can be translated into a curve $\mathcal{J}^{(2)}_{eff}(\omega)$ as shown by the crosses in Figure 7. This curve (where the lowest state of each parity and signature is considered) presents two bumps: they attribute the first one to $i_{13/2}$, $h_{9/2}$ proton alignments and the second one to

the onset of rather large triaxial deformations ($\beta \approx 0.48$, $\gamma \approx 23°$). Although our experimental spectrum does not separate into two peaks at those frequencies (probably because they are averaged over many paths), it certainly has the same average trend for $\mathcal{J}^{(2)}_{eff}$.

SHELL EFFECTS AT HIGH SPINS

The results just presented suggest that single-particle effects still play an important role at high spins in rotational nuclei. As nuclei become less collective, for example, in the lighter erbiums, the definition of $\mathcal{J}^{(2)}_{eff}$ from the height of the γ-ray spectrum becomes more uncertain because of the mixing of stretched dipole and stretched quadrupole transitions. It is also more difficult to apply the feeding correction method because of the increasing lack of correlation between spin and frequency. However, I want to show that we can still learn something about shell effects by looking at the evolution of the continuum spectra in the transition region going towards $N \approx 82$.

Figure 8 shows continuum γ-rays deexciting a population of high spin states (selected by a high total γ-ray energy slice) in ^{160,158,156,154}Er, which are the main (4n) products in the ^{40}Ar-induced compound reactions performed at the 88" cyclotron in Berkeley.[10] There is a rather clear evolution of those spectra from a rather flat one in the rotational nucleus ^{160}Er to a "double bump" structure in ^{154,156}Er nuclei.

The nucleus ^{158}Er is instructive to study because its yrast line is known up to very high spin (~38$\hbar$). In the continuum spectrum, its first backbend is comparable

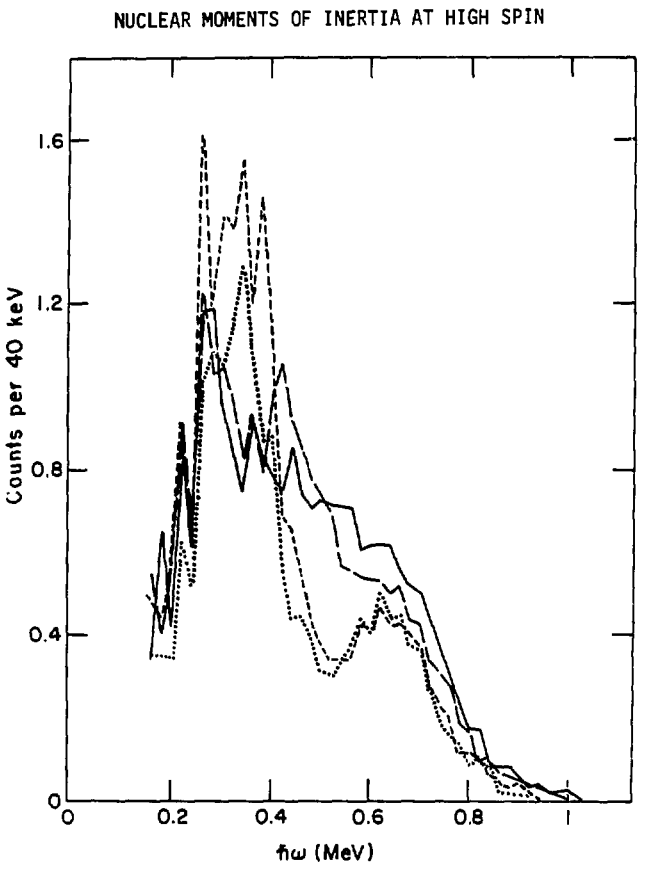

FIGURE 8. Yrast part of the γ-ray "isotropic" spectra (as a function of frequency) deexciting high spins for the following systems: $^{124}Sn + ^{40}Ar$ (solid line), $^{122}Sn + ^{40}Ar$ (long dashed line), $^{120}Sn + ^{40}Ar$ (short dashed line), $^{118}Sn + ^{40}Ar$ (dotted line). The spectra have been normalized to the γ-ray multiplicity and then a "statistical" component has been subtracted.

to that in ^{160}Er but its second backbend is very clear and intense, whereas it is hardly suggested (and not known) in ^{160}Er. This could be due to a change in structure or a change in population flow as a function of neutron number or a combination of them. It is not clear yet what the relative importance of these two factors is. The third backbend is seen as a shoulder around 0.5 MeV. For the observed paths, the upper bump (around 0.6 MeV) is somewhat less intense in ^{158}Er and the intensity missing seems to be shifted down into the lower frequencies (largely into the second backbend) where angular momentum is more easily generated in ^{158}Er than in ^{160}Er. As the neutron Fermi level becomes lower, closer to the beginning of the $h_{9/2}$ and $i_{13/2}$ neutron subshells, the neutrons in those orbitals align more easily. At the same time the ^{158}Er nucleus becomes softer and less collective and can move more easily towards triaxial shapes. This also means that those alignments will occur at lower frequencies.

This trend is expected to continue as the nuclei become more neutron deficient, and indeed it is quite clear in ^{156}Er: the lower energy bump becomes taller and narrower, corresponding to a "compression" of the "valence" backbend frequencies ($\nu i_{13/2}$,$\nu h_{9/2}$,$\pi h_{11/2}$), and in fact Dudek's[11] calculations suggest that the second backbend in that nucleus is due to $h_{9/2}$ neutron alignment. The new feature now is a "dip" at 0.5 MeV between a "low-energy bump" and a "high-energy bump". After the three main backbends of the valence shell have aligned much of the angular momentum available in that shell, the only way to generate angular momentum is by collective motion, which is not very efficient. Then,

at higher frequencies, some new source of alignment occurs. The similarity of all spectra in Figure 8 above 0.6 MeV strongly suggests that alignments of $h_{9/2}, i_{13/2}$ protons from the next shell are the new contributors to angular momentum. The two bumps in ^{156}Er then appear to represent the contributions of two major shells to the angular momentum. This is probably true also for ^{154}Er, although the lower bump is associated with noncollective motion as suggested also by its low proportion of stretched quadrupole transitions (Figure 9).

The evolution of these spectra can therefore be seen as the manifestation of shell effects and of their variation with neutron number. The proton Fermi level is below the N = 5 shell and this favors the $h_{9/2}, i_{13/2}$ particle proton alignment in all those nuclei. As the neutron Fermi level goes up in the valence shell, the (particle-hole) alignments become more difficult and the

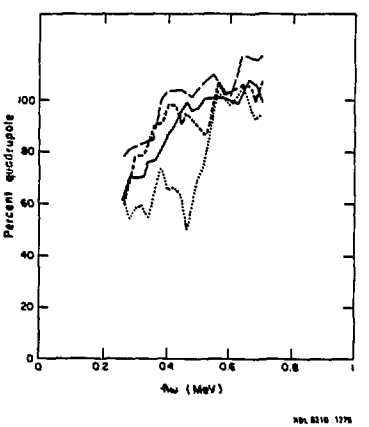

FIGURE 9. Percentage of stretched quadrupole transitions as a function of frequency for the spectra of Figure 8. The systems are represented by the same symbols as in Figure 8.

motion is more collective. A given angular momentum is therefore generated over a wider frequency range than in lighter erbiums. As a consequence, there is no longer a pronounced separation between the two shells in ^{158}Er and ^{160}Er.

CONCLUSION

The realization that a "new" moment of inertia, $\mathcal{J}^{(2)}_{eff}$, can be measured (at least in rotational nuclei) will help in understanding high spin properties of nuclei. It is complementary to $\mathcal{J}^{(2)}_{band}$ and provides a measurement of changes in alignment as a function of frequency. The measurement of $\mathcal{J}^{(2)}_{eff}$ leads to the idea of the separation between alignment and collective angular momentum and the data suggest that shells can be directly separated in continuum γ-ray spectra. A complete separation of shells is seen only in weakly collective nuclei where "valence" alignments are more compressed in frequency, and where the population is closer to the yrast line. This raises the question of temperature effects. Those can probably be best studied in "NaI crystal balls" through combined total γ-ray energy and multiplicity cuts. The push in trying to resolve γ-ray spectra towards higher spins in "Germanium balls" is another approach also likely to reveal detailed behavior at high spins.

This work was supported by the Director, Office of Energy Research, Division of Nuclear Physics of the Office of High Energy and Nuclear Physics of the U.S. Department of Energy under Contract DE-AC03-76SF00098.

NUCLEAR MOMENTS OF INERTIA AT HIGH SPIN

REFERENCES

1. A.W. Sunyar, Physica Scripta, 24, 298 (1981).
2. A. Bohr and B. Mottelson, Physica Scripta, 24, 71 (1981).
3. J. Burde, E.L. Dines, S. Shih, R.M. Diamond, J.E. Draper, K.H. Lindenberger, C. Schuck, and F.S. Stephens, Phys. Rev. Lett., 48, 530 (1982).
4. M.A. Deleplanque, F.S. Stephens, O. Andersen, C. Ellegaard, J.D. Garrett, B. Herkind, D. Fossan, M. Neiman, C. Roulet, D.C. Hillis, H. Kluge, R.M. Diamond, and R.S. Simon, Phys. Rev. Lett., 45, 172 (1980).
5. M.A. Deleplanque, H.J. Körner, H. Kluge, A.O. Macchiavelli, M. Bendjaballah, R.M. Diamond, and F.S. Stephens, submitted to Phys. Rev. Lett.
6. M.A. Deleplanque, Physica Scripta, 24, 158 (1981).
7. G. Leander, Y.S. Chen, and B.S. Nilsson, Physica Scripta, 24, 164 (1981).
8. S. Frauendorf, Physica Scripta, 24, 349 (1981).
9. T. Bengtsson and I. Ragnarsson, Phys. Lett. 115B, 431 (1982).
10. M.A. Deleplanque, R.M. Diamond, E.L. Dines, J.E. Draper, A.O. Macchiavelli, and F.S. Stephens, to be published.
11. J. Dudek, W. Nazarewicz, and Z. Szymanski, Physica Scripta, 24, 309 (1981).